

NUMERICAL SIMULATION OF DIFFERENT ATOMIC NUMBER IONS IRRADIATION EFFECTS ON BENZOCYLOBUTENE MATERIAL

S. X. SUN^{a*}, Y. H. ZHONG^b, R. X. YAO^a, F. J. CHEN^a, Y. X. LI^b

^aHenan Provincial Key Laboratory of Intelligent Lighting, School of Information Engineering, Huanghuai University, Zhumadian 463000, China

^bSchool of Physics and Microelectronics, Zhengzhou University, Zhengzhou 450001, China

In this paper, the irradiation effect of different atomic number incident ions on benzocyclobutene(BCB) material was investigated by using the Monte Carlo method. The results indicated that the projected range of the ions got decreased and the irradiation damage region was moved closer to the surface with the increase of ion atomic number. However, the stopping power was increased with the increase of ion atomic number. Moreover, with the increase of the atomic number, particle distribution, ionization energy loss, vacancies and phonons are more in the irradiation damage zone, the radiation damage mechanism caused by the recoil atoms gradually dominates, and the influence caused by the incident particles is becoming secondary.

(Received July 8, 2020; Accepted October 24, 2020)

Keywords: Benzocyclobutene, Atomic number, Irradiation damage, Energy loss

1. Introduction

With the rapid development of science and technology, semiconductor devices are widely applied in space science such as defense aerospace, satellite remote sensing and so on[1-5]. It is well known that the semiconductor devices are the heart of varieties of electronic system, and when applied in space, they will inevitably be influenced by the irradiation in space[6]. Even if the dose of irradiation in space is low, when the irradiation lasts long enough, the influence will reach a certain value and thus render the device degraded or even dysfunctional, which will impair the stability of the electronic system in space.

In recent years, the research teams at home and abroad have engaged in the study of irradiation hardening. For bulk Si CMOS devices and ICs, the mature irradiation hardening methods have been established, such as gate oxide layer hardness[7] and passivation layer hardness[8]. SOI devices and ICs add the buried oxide layer to improve their irradiation hardness capabilities[9,10]. However, the irradiation reliability of III-V HEMTs was mainly focused on the variation of characteristics and damage mechanism analysis before and after ions radiation. Only few literatures report the structures of irradiation-hardened devices and methods. The method that adopted AlGaN material instead of GaN material as buffer layer to increase the displacement threshold energy and barrier height would suppress the irradiation degeneration degree of GaN

* Corresponding author: sunshuxianga@126.com

HEMTs. But this method would bring the lattice mismatch between material layer, leading to the decrease of the high frequency characteristics of devices. Therefore, depositing the passivation protection layer on exposed area especially the active area has become a feasible way to enhance the irradiation hardening capabilities of HEMTs[11].

Benzocyclobutene (BCB) is a kind of organic passivation material with a low k dielectric and get widely used in HEMT devices[12-14]. It not only can effectively prevent the irradiation ions, avoid the damage of devices, improve the stability of electrical characteristics of semiconductor device, but also can prevent the parasitic capacitance in gate recess region induced by the passivation layer, which can guarantee the high frequency characteristics of devices[14]. In this paper, we have analyzed the impact of irradiation damage of the different atomic number ions with energy range of 10 keV-10 MeV on BCB material. The ions projected range, ions distribution, stopping power and energy loss are investigated in detail using SRIM simulation.

2. Simulations

In numerous particle irradiation simulation software, the SRIM software[15-17] is a relatively mature and widely used one, which is based on Monte-Carlo method. It simulates a large number of ions penetrating into the target and tracks its motion process, then stores the various parameters such as the location of the incident ions, energy loss, secondary ions and so on. SRIM software adopts continuous slowing-down hypothesis in calculation process, namely the collisions between the incident ions and the target nuclear using the two body collision method. This part mainly caused the twists and turns of the incident ions trajectory, the energy loss due to the section of elastic energy loss and the two two-body collision. It is supposed that the incident ions interact with the electrons in the material to lose energy continuously and uniformly, and the distance between the two-body collision and the parameters after collision are obtained by random sampling.

In this paper, different ions, such as H, He, B, C, Fe, Cu, Au, Ag, Pt, U with the number of the 10^5 penetrating into BCB material were studied. The mean projected range of ions H, He, B, C, Fe, Cu, Au, Ag, Pt, U ranging from 10keV to 10MeV in BCB has been calculated by using the SR module, as shown in Fig. 1. The Fig.1 shows that the mean projected ranges of different incident ions increase as the incident energy increases. But for the same incident energy, the smaller the atomic number for the ion is, the greater the mean projected range will be. It is obvious that if we draw a straight line perpendicular to the horizontal axis, a straight line parallel to horizontal axis has been curved similarly. there is no doubt that for the same projected range, the greater the number of atoms get, the higher the incident energy will be. Therefore, for the degree of penetration on BCB material, $H > B > C > Fe > Cu > Ag > Pt > Au > U$.

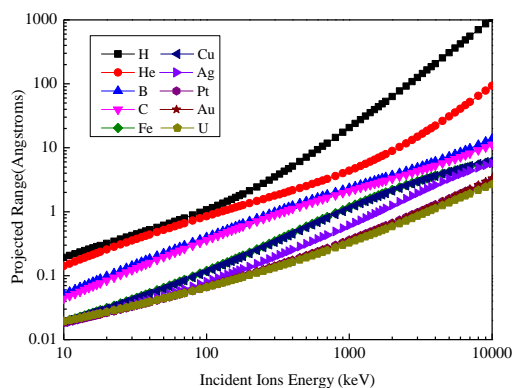


Fig.1. The projected range of different atomic number ions in BCB material with incident energy variation from 10 keV to 10MeV.

3. Results and discussion

The range of the incident particles (R_p) in the incident direction and the end position in the target object intuitively reflect its irradiation damage to the material. In this paper, the distributions of different particles at 1MeV in BCB are investigated, as shown in Fig. 2. Obviously, with the increase of atomic number, the aggregation area of particles moves gradually from the interior to the surface, and peaks exist in the distributions. The number of particles around the peak region is very small, which satisfies the Bragg peak distribution. The peak width gradually increases, indicating that the range of the standard deviation (ΔR_p) gradually increases. At the same time, it is noticed that the peak value increases with the increase of atomic number except for Fe, Cu and Ag, which is not only related to the incident energy, but also to the stopping power of the target material to the particles. The stopping power can be described by the energy loss ($-dE/dX$) of the incident particle in the unit path and it is divided into the electronic stopping power and the nuclear stopping power[15]. The electron stopping power reflects the energy loss induced by the excitation and ionization when the proton collides with the outside of the nucleus of the lattice. The nuclear stopping power reflects the energy loss caused by the proton colliding with the target nucleus. Figure 3 is the stopping power calculated by particles mentioned above. When the energy is below 1MeV, the electronic stopping power of Fe, Ag and Cu gradually decrease and the nuclear stopping power increase first and then decrease; Furthermore, for the same incident energy, the greater the mass of incident particle is, the smaller the speed will be. Therefore, the range of light particles are longer than heavy particles.

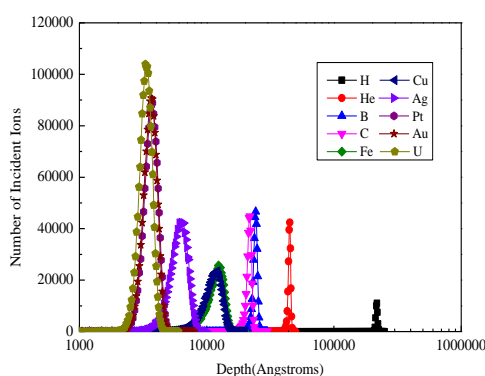


Fig. 2. The different atomic number ions distribution in BCB material with incident energy 1MeV.

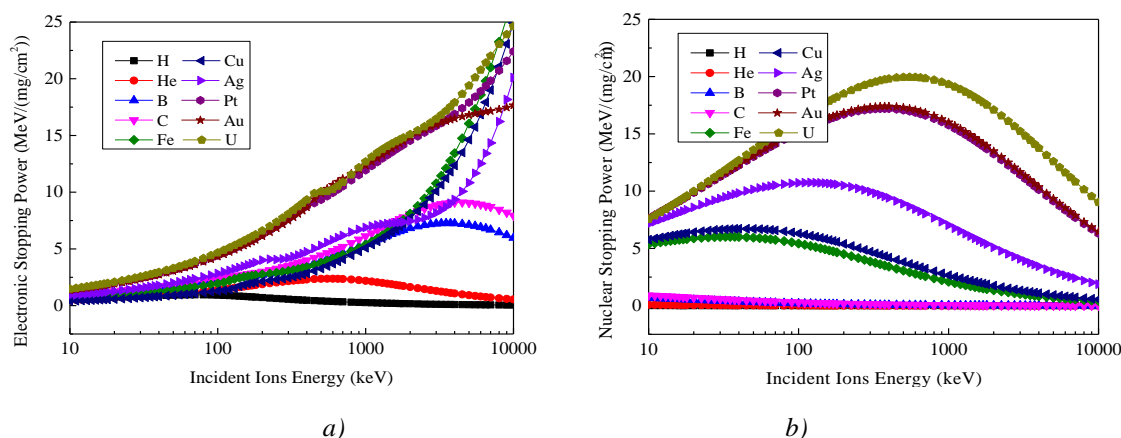


Fig. 3. (a) nuclear stopping power and (b) electronic stopping power of different atomic number ions in BCB material with incident energy variation from 10 keV to 10MeV.

The cumulative energy loss of the incident particles include the ionization energy loss (IEL) and non-ionizing energy loss (NIEL). Relative research has showed that there exists a good linear relationship between non-ionizing energy deposition of devices and non-ionizing radiation damage of devices in most cases while it is quite different for different particles[18]. The particles transfer energy to the electron in the target, in which a number of target atoms are inspired or ionized and the energy loss of this process is called electron energy loss and corresponding irradiation effect is named as the ionization effect. Vacancy is an empty lattice position induced by replacement collision and the number of vacancies determines the degree of the degradation of materials. The phonon is the lattice vibration's normal mode of energy quantum, used to describe harmonic vibration of crystal lattice. The ionization energy loss, vacancies distribution, phonons distribution, and their percentage of energy occupied by the incident particles in BCB are shown in Fig. 4-6. They are composed of two parts, the one is caused by incident particles, the other one is caused by recoil atoms. For the ionization energy loss, the numerical value drops sharply at the end of the particle path. With the increase of atomic number, the energy loss of ionization gradually shifts from the interior to the surface, and the influence of the incident particles increased gradually, instead, the influence of recoil atoms decreased gradually. However, for the atom with a smaller atomic number such as H, He, B, C, Fe and Cu, the trend of change is more rapid and for the larger atomic number such as Ag, Pt, Au and U, the trend is relatively gentle. For the distribution of vacancies and phonons, both slowly increase after the rapid decline with increasing incident depth. The bigger the atomic number is, the more widely the vacancies and phonons will be distributed on the surface of BCB. While the energy loss caused by the incident particles and recoil atoms first increases rapidly and then tends to be gentle, but the influence of recoil atoms was dominant and the that of the incident particles is secondary. In summary, the irradiation damage region caused by different particles at 1MeV on BCB gradually moves toward the material surface as the atomic number increases, and the impact of recoil atoms is becoming dominant.

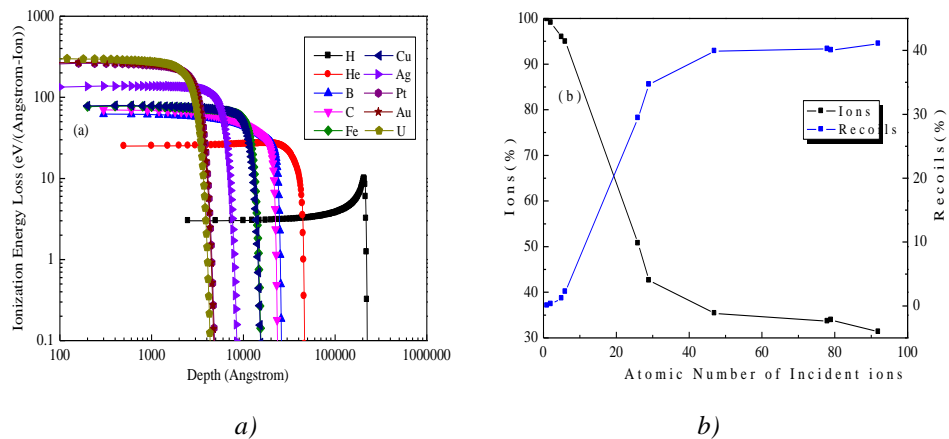


Fig. 4. The ionization energy loss (a) and energy loss percentage due to ionization (b) for 1 MeV different atomic number ions.

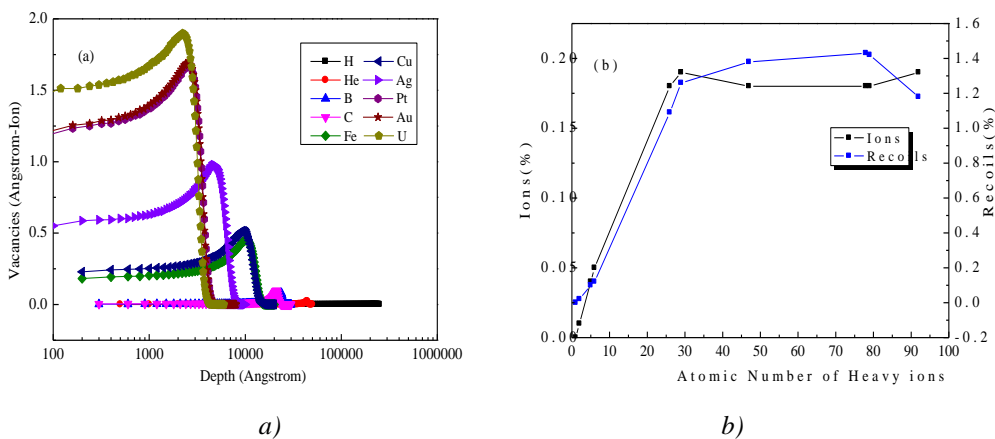


Fig. 5. The vacancies distribution (a) and energy loss percentage due to vacancies (b) for 1 MeV different atomic number ions.

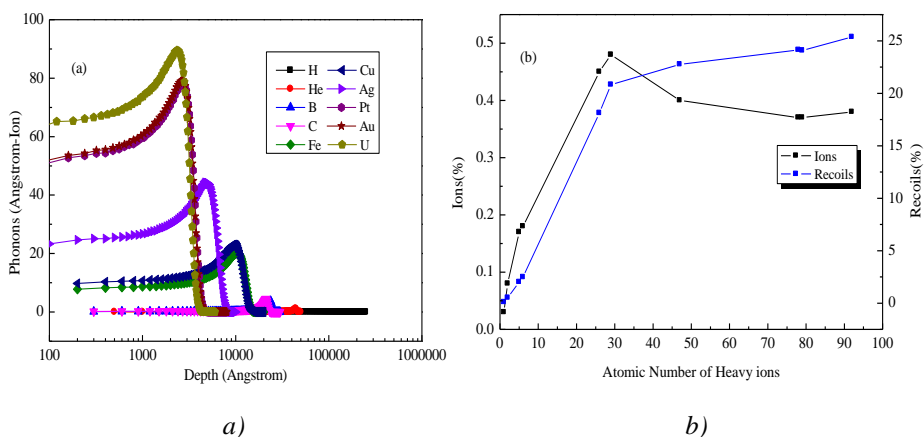


Fig. 6. The phonons distribution (a) and energy loss percentage due to phonons (b) for 1 MeV different atomic number ions.

4. Conclusions

In this paper, the projected range, particle distributions, ionization energy loss, vacancies and phonons distribution of different ions such as H, He, B, C, Fe, Cu, Ag, Pt, Au, U with the number of 10^5 radiating on BCB material were calculated. The calculation results indicate that the permeability of BCB is stronger for the smaller atomic number particle such as H, He, B, C, Fe and Cu, and the irradiation damage region is mainly concentrated in the interior of the material and the irradiation damage zone moves closer to the surface part of the material with a larger atomic number, Ag, Pt, Au, U. With the increase of the atomic number, particle distribution, ionization energy loss, vacancies and phonons are more in the irradiation damage zone, the radiation damage mechanism caused by the recoil atoms gradually dominates, and the influence caused by the incident particles is becoming secondary.

Acknowledgements

The authors would like to express heartfelt thanks to P. H. Xia from Zhejiang University of China for guidance in the operation software. This research was funded by the National Natural Science Foundation of China (No. 11775191), Promotion Funding for Excellent Young Backbone Teacher of Henan Province in China (2019GGJS017), Henan International Joint Laboratory of Behavior Optimization Control for Smart Robots, file No. [2018]19.

References

- [1] O. Zaoui, N. Dahbi, L. Ayat, *Journal of Ovonic Research*, **16**(1), 29 (2020).
- [2] A. Stocco, S. Gerardin, D. Bisi, S. Dalcanale, F. Rampazzo, M. Meneghini, G. Meneghesso, J. Grünenpütt, B. Lambertc, H. Blanck, E. Zanon, *Microelectronics Reliability* **54**, 2213 (2014).
- [3] H. Y. Kim, C. F. Lo, L. Liu, F. Ren, J. Kim, S. J. Pearton, *Applied Physics Letters* **100**, 012107 (2012).
- [4] K. M. K. H. Leong, X. B. Mei, W. Yoshida, P. Liu, Z. Zhou, M. Lange, L. Lee, J. G. Padilla, A. Zamora, B. S. Gorospe, K. Nguyen, W. R. Deal, *IEEE Microwave and Wireless Components Letters* **25**(6), 397 (2015).
- [5] P. Carniti, L. Cassina, C. Gotti, M. Maino, G. Pessina, *Nuclear Instruments and Methods in Physics Research A* **824**, 258 (2016).
- [6] L. Lv, J. G. Ma, Y. R. Cao, J. C. Zhang, W. Zhang, L. Li, S. R. Xu, X. H. Ma, X. T. Ren, Y. Hao, *Microelectronics Reliability* **51**, 2168 (2011).
- [7] B. L. Draper, M. R. Shaneyfelt, R. W. Young, T. J. Headley, R. Dondero, *IEEE Transactions on Nuclear Science* **52**(6), 2387 (2005).
- [8] Y. D. Zhao, D. Q. Li, L. Xiao, J. K. Liu, X. Y. Xiao, G. H. Li, Y. H. Jin, K. L. Jiang, J. P. Wang, S. S. Fan, Q. Q. Li, *Carbon* **108**, 363 (2016).
- [9] Z. S. Zheng, J. Ning, B. Q. Zhang, Z. L. Liu, J. J. Luo, Z. S. Han, *Science China Materials* **59**(8), 657 (2016).
- [10] Z. E. Xia, Q. Cong, Z. Z. Xuan, L. L. Cheng, W. Xi, W. Y. Min, W. X. He, Z. G. Ru,

- E. Y. Fei, L. H. Wei, S. Qian, *Chinese Physics B* **15**(4), 792 (2006).
- [11] A. D. Koehler, T. J. Anderson, M. J. Tadjer, B. D. Weaver, J. D. Greenlee, D. I. Shahin, K. D. Hobart, F. J. Kub, *IEEE Electron Device Letters* **37**(5), 545 (2016).
- [12] C. L. Tan, H. Wang, K. Radhakrishnan, *IEEE Transactions on Device and Materials Reliability* **7**(3), 488 (2007).
- [13] S. Ozaki, K. Makiyama, T. Ohki, Y. Kamada, M. Sato, Y. Niida, N. Okamoto, S. Masuda, K. Joshin, *Phys. Status Solidi A* **212**(5), 1153 (2015).
- [14] X. Lu, J. Ma, H. X. Jiang, C. Liu, P. Q. Xu, K. M. Lau, *IEEE Transactions on Electron Devices* **62**(6), 1862 (2015).
- [15] H. Korkut, T. Korkut, A. Kara, M. Yigit, E. Tel, *Journal of Fusion Energy* **35**, 591 (2016).
- [16] H. Korkut, T. Korku, *Journal of Radioanalytical Nuclear Chemistry* **299**, 13 (2014).
- [17] N. Dahbi, R. B. Taleb, O. Zaoui, *Journal of Ovonic Research* **15**(3), 167 (2019).
- [18] G. P. Summers, E. A. Burke, P. Shapiro, S. R. Messenger, R. J. Walters, *IEEE Transactions on Nuclear Science* **40**(6), 1372 (1993).